Effects of the interplay of neighboring couplings on the possible phase transition of a two-dimensional antiferromagnetic system

Ai-Yuan Hu[1] and Huai-Yu Wang[2,*]

[1]*College of Physics and Electronic Engineering, Chongqing Normal University, Chongqing 401331, China*

[2]*Department of Physics, Tsinghua University, Beijing 100084, China*

(Received 1 May 2016; published 26 July 2016)

We investigate the phase transition of the quantum spin-1 anisotropic antiferromagnet on a square lattice. The model is described by the Heisenberg Hamiltonian with the nearest-neighbor coupling strengths J_{1a} and J_{1b} along the x and y directions, respectively, and next-nearest-neighbor coupling J_2. This model allows Néel state (AF1) and collinear state (AF2). The effects of the spatial and single-ion anisotropy on phase transformation between these two states are explored. Our results show that the two states can exist and have the same critical temperature at $D > 0$ as long as $J_2 = J_{1b}/2$. Under such parameters, a first-order phase transformation between these two states below the Néel point can occur when J_{1b} value is not very small and D value is within a narrow range. For $J_2 \neq J_{1b}/2$, although both states may exist, their Néel temperatures differ. If the Néel point of the AF1 (AF2) state is larger, then at very low temperature, the AF1 (AF2) state is more stable. Thus, in an intermediate temperature, a first-order phase transition between these two states may occur.

DOI: 10.1103/PhysRevE.94.012142

I. INTRODUCTION

Over the past two decades, much attention has been paid to study the magnetic properties of frustration in the two-dimensional (2D) quantum Heisenberg model (known as the J_1-J_2 model) with competing nearest-neighbor (NN) antiferromagnetic exchange interaction J_1 and next-nearest-neighbor (NNN) J_2 [1]. This is because some real materials can be described by such a model [2–7]. Examples are the undoped precursors to the high temperature superconducting cuprates for small J_2/J_1 values [2], $VOMoO_4$ for intermediate J_2/J_1 values [3], and Li_2VOSiO_4 for large J_2/J_1 values [4]. For Li_2VOSiO_4, nuclear magnetic resonance, magnetization, specific heat, and muon spin-rotation measurements revealed significant coupling between NN and NNN neighbors [5–7]. Experimental investigations indicated that its ground-state phase diagram could be explored from low J_2/J_1 to high by applying high pressures [5]. x-Ray diffraction measurements on this compound showed that the value of J_2/J_1 decreased by about 40% when pressure increased from zero to 7.6 GPa [5]. In addition, these experiments on Li_2VOSiO_4 showed that it underwent a phase transition at a low temperature (2.8 K) to a collinear antiferromagnetic order with magnetic moments lying in the a-b plane with $J_2 + J_1 \sim 8.2$ K and $J_2/J_1 \sim 1.1$ [3,6,7].

The J_1-J_2 model is also of theoretical interest. The investigations indicated that at zero temperature, three cases could appear depending on the parameter $\alpha = J_2/J_1$ [8–13]. For $\alpha < \alpha_1 \sim 0.38$ the system was the Néel state with wave vector $Q = (\pi,\pi)$ (AF1) and for $\alpha > \alpha_2 \sim 0.6$ the system was the collinear state degenerate with pitch vectors $Q = (\pi,0)$ and $(0,\pi)$ (AF2). These two degenerate collinear states were characterized respectively by a parallel spin orientation of NN in the vertical (or horizontal) direction and an antiparallel spin orientation of NN in the horizontal (or vertical) direction. For $\alpha_1 < \alpha < \alpha_2$, there was a nonmagnetic gapped phase [14,15]. The nature of the ground state of this model turned out to be one of the most challenging problems for physics of frustrated spin systems [8–13]. One may think that the spin-liquid state was the most promising candidate [16].

For finite temperature, when an Ising type anisotropy is considered, there will be Chandra-Coleman-Larkin transition and Berezinskii-Kosterlitz-Thouless transition [17], where the anisotropy plays a role.

Some discussions were represented about the quantum phase transition for this model by Bishop *et al.* [18]. They thought that "frustrated models often exhibit accidental degeneracy, and the degeneracy degree could vary enormously, has been widely viewed as a measure of the frustration. Among the effects that can act to lift any such degeneracy are quantum and thermal fluctuations" [18].

A generalization of the frustrated J_1-J_2 model is the J_{1a}-J_{1b}-J_2 model [19–24]. It possesses more degrees of freedom to tune the fluctuation of system compared to the J_1-J_2 model, since the NN exchange interactions J_{1a} and J_{1b} along the x and y directions in this model are of different strengths. This feature leads naturally to an increased sensitivity of the underlying Hamiltonian to the presence of small perturbations.

Our primary purpose of this work is to study the phase transition of the J_{1a}-J_{1b}-J_2 model at finite temperature by using the double-time Green's function method. The effect of anisotropy on the stabilization of Néel and collinear states are discussed in detail. We study two cases separately as J_{1a} is fixed. One is that as $J_2 = J_{1b}/2$, both the Néel state and collinear state can exist and have the same Néel temperature. The other is that as $J_2 \neq J_{1b}/2$, the two states can also exist, but their Néel points are not the same. For these two cases, a phase transformation between Néel and collinear states below the Néel point may occur. Which of the states is more stable depends on the spatially and single-ion anisotropies of the system.

Here we would like to mention that the ground state of the 2D antiferromagntic system has been studied by many researchers. For instance, the exact ground-state phase diagram of the Potts model was given by Takasaki *et al.* [25]. In the

*wanghuaiyu@mail.tsinghua.edu.cn

present work, we care the cases of finite temperature, and the ground state will not be touched.

This paper is organized as follows. In Sec. II, we introduce the theoretical model and present the formulism of Green's function to derive the self-consistent equation for evaluation of magnetizations. In Sec. III, the numerical results are presented and discussed. Section IV is our concluding remarks.

II. MODEL AND METHOD

We consider a 2D spatial anisotropy J_{1a}-J_{1b}-J_2 model with easy-axis single-ion anisotropy. The model is described by the following Hamiltonian:

$$\begin{aligned} H = {} & J_{1a}\sum_{\langle i,j\rangle}\left[\left(S_i^x S_j^x + S_i^y S_j^y\right) + S_i^z S_j^z\right] \\ & + J_{1b}\sum_{\langle i,j\rangle}\left[\left(S_i^x S_j^x + S_i^y S_j^y\right) + S_i^z S_j^z\right] \\ & + J_2\sum_{[i,j]}\left[\left(S_i^x S_j^x + S_i^y S_j^y\right) + S_i^z S_j^z\right] - D\sum_i \left(S_i^z\right)^2, \end{aligned} \quad (1)$$

where S_i^x, S_i^y, and S_i^z represent the three components of the spin-S operator for a spin at site i. The sums $\langle i,j\rangle$ and $[i,j]$ run over the NN and NNN lattice sites, respectively. J_{1a} and J_{1b} represent the NN exchange parameters along the x and y directions, respectively. J_2 is the NNN exchange parameter. D denotes the single-ion anisotropic parameter. In this paper, our primary attention is focused on studying the phase transition of the 2D square lattice frustrated Heisenberg antiferromagnet at finite temperature. If this system has no anisotropy, there is no long-range order at finite temperature [26]. Therefore, an anisotropy is necessary.

For the sake of convenience, we let Boltzmann constant $k_B = 1$ so all the quantities, including Hamiltonian parameters, temperature T, and sublattice magnetization $m = \langle S^z\rangle$, become dimensionless. $\langle S^z\rangle$ is the assembly statistical average of spin operator S^z. We fix $J_{1a} = 1$ and change the J_{1b} and J_2 values in computation.

We apply the double-time Green's function method to deal with the Hamiltonian (1). The Green's function is defined as follows:

$$G_{ij}^{\pm} = \left\langle\!\left\langle S_i^{\pm}; e^{uS_j^z} S_j^{-}\right\rangle\!\right\rangle. \quad (2)$$

Here, u is a parameter [27]. After solving the Green's function by means of the method of equation of motion, u will be ultimately set as zero to give the expression of magnetization [27]. We derive the equation of the motion of the Green's function by standard procedure [27]. In this course, the higher-order Green's functions have to be decoupled. For the terms concerning exchange interaction in Eq. (1), we use a Tyablikov or random-phase approximation decoupling [27]:

$$\left\langle\!\left\langle S_l^z S_i^{\pm}; e^{uS_j^z} S_j^{-}\right\rangle\!\right\rangle = \left\langle S_l^z\right\rangle\left\langle\!\left\langle S_i^{\pm}; e^{uS_j^z} S_j^{-}\right\rangle\!\right\rangle; l \neq i. \quad (3)$$

For the terms concerning the single-ion anisotropy, we adopt the Anderson-Callen's decoupling [28]:

$$\left\langle\!\left\langle S_i^z S_i^{+} + S_i^{+} S_i^z; e^{uS_j^z} S_j^{-}\right\rangle\!\right\rangle = 2C_1\left\langle S_i^z\right\rangle\left\langle\!\left\langle S_i^{+}; e^{uS_j^z} S_j^{-}\right\rangle\!\right\rangle, \quad (4)$$

where

$$C_1 = 1 - \frac{1}{2S^2}\left[S(S+1) - \left\langle\left(S_i^z\right)^2\right\rangle\right]. \quad (5)$$

This decoupling form has been widely used, and it is applicable to any spin quantum number [29]. Because of the decoupling approximations Eqs. (4) and (5), the partition function with respect to temperature may not be well represented. We adopt them because they have been generally accepted. These approximations are applicable at finite temperature, but not good enough for zero temperature, so we will not investigate the ground state.

The Green's function is Fourier transformed into wave vector space, and the correlation function $\langle e^{uS_i^z} S_i^{-} S_i^{+}\rangle(k)$ is calculated via the spectral theorem [27,29]. Let us define

$$\frac{2}{N}\sum_k \left\langle e^{uS_i^z} S_i^{-} S_i^{+}\right\rangle(k) = \theta(u)\phi_F, \quad F = \mathrm{AF1}, \mathrm{AF2}, \quad (6)$$

where the summation of wave vector k runs over the first Brillouin zone. N is the number of lattice sites and

$$\theta(u) = \left\langle\left[S_i^{+}, e^{uS_j^z} S_j^{-}\right]\right\rangle. \quad (7)$$

Now we let $u = 0$, as has been mentioned above. This leads to $\theta(0) = 2m$ and

$$\phi_F = \frac{2}{N}\sum_k \frac{E_{1F}}{2\sqrt{E_{1F}^2 - E_{2F}^2}} \coth\frac{\sqrt{E_{1F}^2 - E_{2F}^2}}{2T} - \frac{1}{2}. \quad (8)$$

Here for the AF1 state,

$$\begin{aligned} E_{1\mathrm{AF1}} = {} & 2m\Big\{2J_2(\cos k_x \cos k_y - 1) + (J_{1a} + J_{1b}) \\ & + D\left[1 - \frac{m(1+2\phi_{\mathrm{AF1}})}{2S^2}\right]\Big\}, \\ E_{2\mathrm{AF1}} = {} & 2m(J_{1a}\cos k_x + J_{1b}\cos k_y), \end{aligned} \quad (9)$$

and for the AF2 state,

$$\begin{aligned} E_{1\mathrm{AF2}} = {} & 2m\Big\{J_{1b}(\cos k_y - 1) + (J_{1a} + 2J_2) \\ & + D\left[1 - \frac{m(1+2\phi_{\mathrm{AF2}})}{2S^2}\right]\Big\}, \\ E_{2\mathrm{AF2}} = {} & 2m(J_{1a}\cos k_x + 2J_2\cos k_x \cos k_y). \end{aligned} \quad (10)$$

Using Eqs. (7) and (8) and the relation $\langle S_i^{-} S_i^{+}\rangle = S(S+1) - \langle S_i^z\rangle - \langle (S_i^z)^2\rangle$, the sublattice magnetization is expressed by following formula [27,29]:

$$m = \frac{(\phi_F + 1 + S)\phi_F^{2S+1} - (\phi_F - S)(\phi_F + 1)^{2S+1}}{(\phi_F + 1)^{2S+1} - \phi_F^{2S+1}}. \quad (11)$$

III. RESULTS AND DISCUSSIONS

In this paper, the properties of the J_{1a}-J_{1b}-J_2 model at finite temperature are investigated. Therefore, when we say "zero temperature," we actually mean that the temperature is very close to zero, which is denoted by $T = 0^+$.

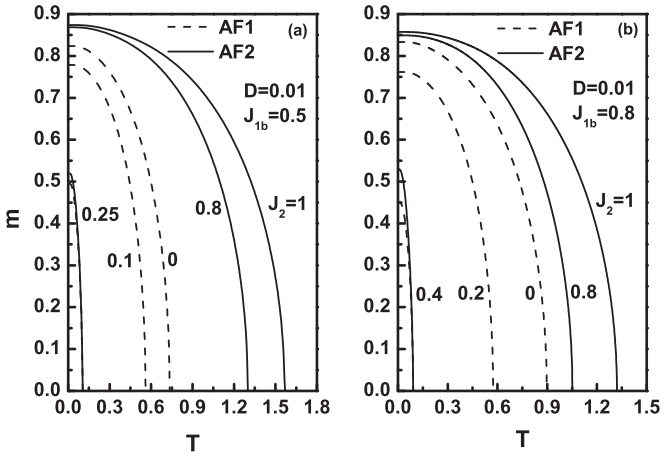

FIG. 1. The sublattice magnetization m as a function of temperature T for different J_2 values when $D = 0.01$. (a) $J_{1b} = 0.5$ and (b) $J_{1b} = 0.8$.

A. Magnetic properties

Figure 1 plots the magnetization m as a function of temperature for different J_{1b} and J_2 values. In Fig. 1(a), $J_{1b} = 0.5$. The m decreases as J_2 approaches 0.25 from either side. This is the result of the competition between J_2/J_{1a} and J_{1b}/J_{1a}. Since we have fixed $J_{1a} = 1$, this competition is actually between J_2 and J_{1b}. As $J_2 = 0$, the Hamiltonian is a two-dimensional antiferromagnetic model with only NN exchange interactions. When J_2 increases from 0, the frustration is increased. The competition between J_2 and J_{1b} emerges, and it will increase with increasing J_2 for fixed J_{1b}. Therefore, the magnetization and critical temperature drop with increasing J_2. At $J_2 = 0.25$, the competition reaches the strongest. It is an AF1 state in the range of $0 \leqslant J_2 \leqslant 0.25$. As J_2 further increases from 0.25, the competition becomes gradually weaker. The role of J_2 becomes more important. As a result, both magnetization and critical temperature increase. It is an AF2 state in the range of $J_2 \geqslant 0.25$. In one word, $J_2 = J_{1b}/2$ is a boundary value of AF1 and AF2 configurations. Figure 1(b) gives another example for $J_{1b} = 0.8$, where the boundary value is $J_2 = 0.4$.

The description above is the case of finite temperature. For temperature closing to zero, it is seen that the value of $m_{\mathrm{AF1}}(0^+)$ is less than $m_{\mathrm{AF2}}(0^+)$. This can be easily explained. For AF1 configuration, each spin is antiparallel to all of its four NN spins, while in the AF2 configuration each spin has two parallel and two antiparallel NN spins. Therefore, the AF1 state has stronger quantum fluctuation than the AF2 state. This leads to $m_{\mathrm{AF1}}(0^+) < m_{\mathrm{AF2}}(0^+)$ near zero temperature. Similarly, we can understand that the difference between $m_{\mathrm{AF1}}(0^+)$ and $m_{\mathrm{AF2}}(0^+)$ increases with the increase of J_{1b} at $J_2 = J_{1b}/2$, see Figs. 1(a) and 1(b). A bigger J_{1b} value is corresponding to a stronger quantum fluctuation for AF1 and a weaker quantum fluctuation for AF2. It is noted that, for AF1, the frustration is the least at $J_2 = 0$. For AF2, although the frustration is weaker, it actually exists. The NNN spins may also play a role in causing frustration, but, intuitively, not so important as the NN ones.

Comparing Figs. 1(a) and 1(b), two points need to be stressed. (1) The critical temperature increases with decreasing J_{1b}. (2) The two states with the same parameters have the same critical temperature as long as $J_2 = J_{1b}/2$. In order to show these two points more explicitly, Fig. 2 plots the phase diagrams.

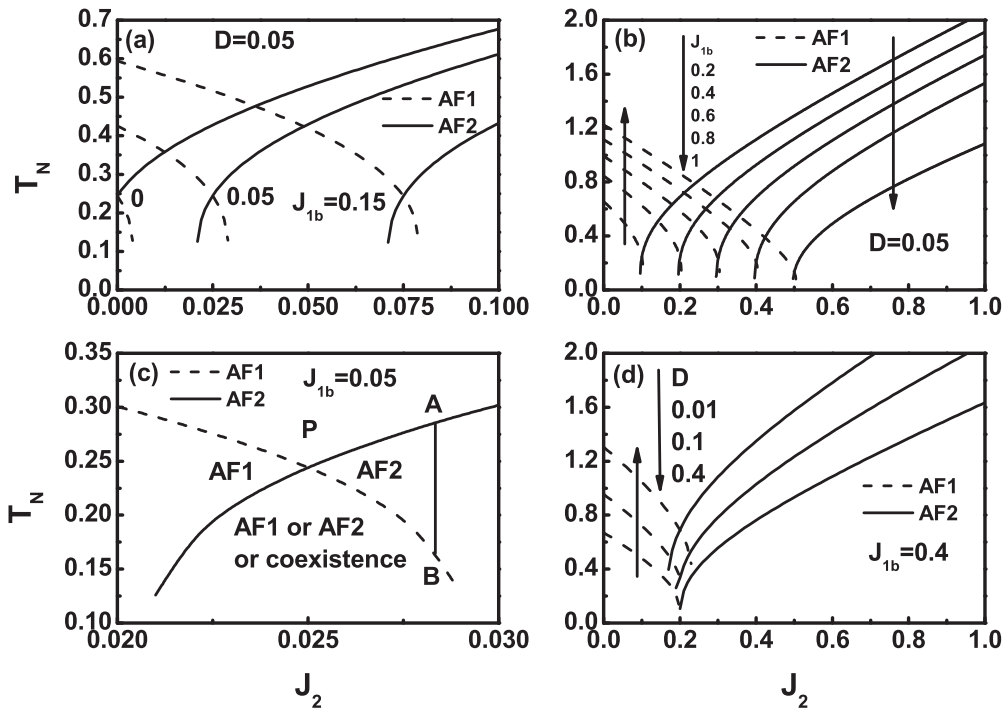

FIG. 2. The Néel temperature T_N as a function of J_2 for $D = 0.05$ when the J_{1b} increases from 0 to 1. (a) $J_{1b} = 0$, 0.05, and 0.15; (b) $J_{1b} = 0.2$, 0.4, 0.6, 0.8 and 1. The left and right arrows represent the J_{1b} from smaller to larger values for AF1 and AF2, respectively. (c) The enlargement of the region of J_2 in the vicinity of $J_2 = 0.025$ when $J_{1b} = 0.05$; (d) the Néel temperature T_N as a function of J_2 for $J_{1b} = 0.4$ when $D = 0.01, 0.1$ and 0.4. The left and right arrows represent the D from smaller to larger for AF1 and AF2, respectively.

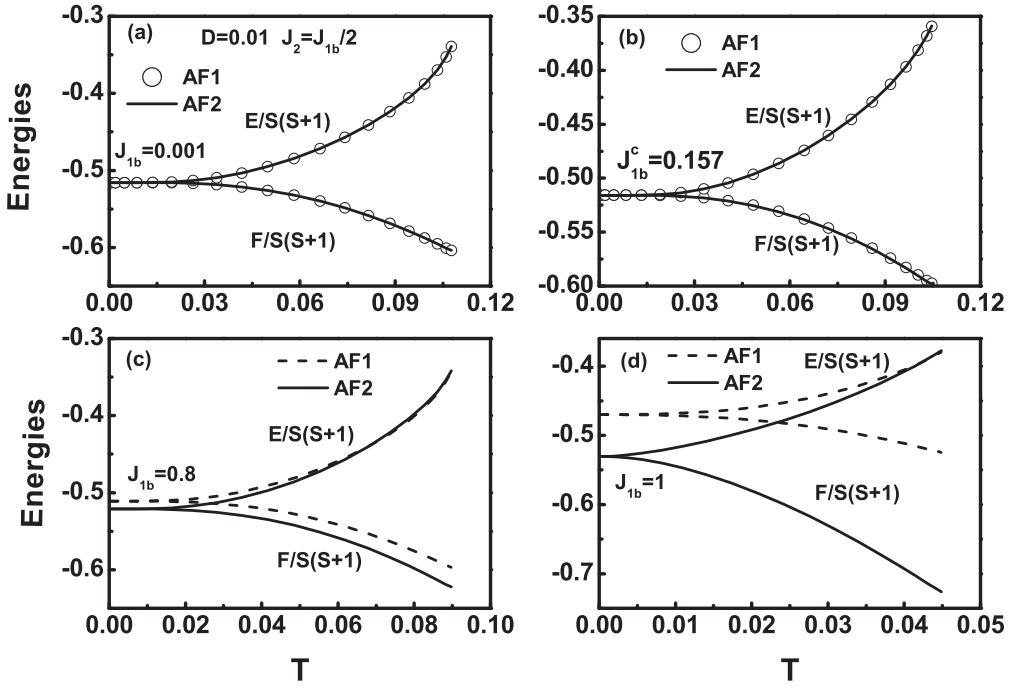

FIG. 3. The internal energies $E(T)$ (ascending lines) and free energies $F(T)$ (descending lines) as a function of temperature T at $D = 0.01$. (a) $J_{1b} = 0.001$, (b) $J_{1b} = 0.157$, (c) $J_{1b} = 0.8$, and (d) $J_{1b} = 1$.

Figure 2(a) plots the critical temperature as a function of J_2 for a number of J_{1b} values. As $J_{1b} = 0$ and $J_2 = 0$, both AF1 and AF2 recover an ordinary one-dimensional single-ion anisotropic Heisenberg antiferromagnetic model. As a consequence, they have the same critical temperature. For AF1 state, as J_{1b} increases from 0, the competition between J_{1b} and J_2 becomes weaker, which leads to rise of the T_N. The AF2 state is just a contrary case, i.e., the competition between J_{1b} and J_2 becomes stronger with increasing J_{1b}, which results in the drop of T_N. Due to these two reasons, the cross point of the critical temperature curves of the two states shifts rightwards with increasing J_{1b}, see Figs. 2(a) and 2(b). Nevertheless, the slops of the critical temperatures of the two states becomes more and more slower with increasing J_{1b} except near $J_2 = J_{1b}/2$, see Figs. 2(a) and 2(b). It leads to the drop of cross point of the critical temperature between AF1 and AF2. Accordingly, the temperature corresponding to the cross point decreases with the increase of J_{1b}, agreeing with Fig. 1. This is actually caused by the competition between J_{1b} and J_2.

In Fig. 2, the critical temperature curves of the two states cross. To be explicit, Fig. 2(c) is the enlargement of Fig. 2(a) when J_2 is in the vicinity of 0.025 for $J_{1b} = 0.5$. In this panel, the J_2 values of points A and B are the same, although in different states. The two curves in Fig. 2(c) divide the region into four regions: The upper region is paramagnetic state (P); the left and right regions are AF1 and AF2 state, respectively; the lower region can be the coexistence of AF1 and AF2.

Figure 2(d) plots the critical temperature as a function of J_2 for different D values when $J_{1b} = 0.4$ and $J_2 = J_{1b}/2$. The two states have the same critical temperature at $D > 0$ as long as $J_2 = J_{1b}/2$. For larger D values, the two critical temperature curves cross. This is because the anisotropy suppresses the frustration of the system. The stronger the anisotropy, the weaker the frustration. The corresponding crossing range becomes larger and vice versa. Consequently, the critical temperature increases with increasing D, and the temperature corresponding the intersection point rises. As D becomes faint, the crossing area disappears.

It is noted in Fig. 2 that, no matter what the value of other parameters are, AF1 and AF2 have the same critical temperature for $D > 0$ as long as $J_2 = J_{1b}/2$. Since both configurations are possible, one may ask which one is more stable. In the following, this problem will be discussed in detail. Before that we note that at $J_{1b} = 0$ and $J_2 = 0$, the system actually becomes the array of uncoupled one-dimensional chains. Therefore, the case of $J_{1b} = 0$ shall be not discussed.

For two states under the same volume and entropy, the one with lower internal energy is more stable. However, their entropies differ at a fixed temperature. Therefore, the internal energy cannot be used to determine which one is more stable at a temperature. Under the same volume and temperature, the state with lower free energy is more stable.

The free energy can be evaluated numerically by means of the internal energy via $F(T) = E(0) - T\int_0^T \frac{E(T')-E(0)}{T'^2}dT'$, where $E(T)$ represents the internal energy of the system, which is defined as the thermostatistical average of Hamiltonian, $E = \frac{\langle H\rangle}{N}$ [29]. Computing internal energy involves the calculation of the transverse $(\sum_{i,j}\langle S_i^+ S_j^-\rangle)$ and longitudinal $(\sum_{i,j}\langle S_i^z S_j^z\rangle)$ correlation functions. We do not present the lengthy derivation of their expressions recently developed. Please refer to Ref. [30]. As mentioned above, the used decoupling approximation lead to the fact that the partition function with respect to temperature may not be well represented. We are aware of this shortcoming. Better approximations are still being explored. In this paper, we mainly compare the free energies of the two states. Since they are computed under the

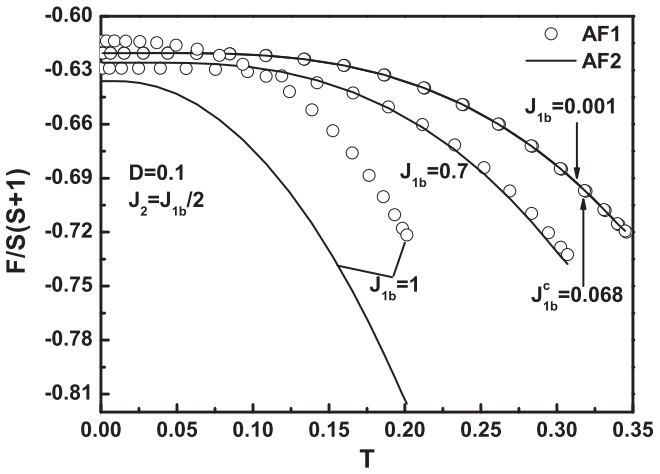

FIG. 4. The free energies $F(T)$ as a function of temperature T for different J_{1b} values when $D = 0.1$.

same approximation, it is believed that the relative values are meaningful. Please note that in this paper, we calculate the free energy below the Néel point T_N.

B. Possible phase transition at $J_2 = J_{1b}/2$

Figure 3 plots the energies as a function of temperature for different J_{1b} values when $J_2 = J_{1b}/2$ and $D = 0.01$. For $E(T)$, it increases with temperature monotonically, as it should be, while the free energies $F(T)$ decrease with temperature monotonically. As J_{1b} increases from 0 to 0.157, the energy differences between the two states are negligible. Figures 3(a) and 3(b) show two examples with $J_{1b} = 0.001$ and 0.157, respectively. This means that the system can be in either the AF1 or AF2 state or a coexistence of them. For convenience, we denote $J^c_{1b} = 0.157$. When J_{1b} further increases from J^c_{1b}, F_{AF1} deviates gradually from F_{AF2}. The difference between them increases with increasing J_{1b}, see Figs. 3(c) and 3(d). Meanwhile, the curve of F_{AF2} drops faster than F_{AF1}. Moreover, F_{AF2} is always lower than F_{AF1} within the whole temperature range below the Néel point. Hence, in this case, the AF2 state is more stable.

Figure 3 discusses the case of a weaker anisotropy. Figure 4 plots the free energy as a function of temperature for a stronger anisotropy. There is also a J^c_{1b} value. When $0 < J_{1b} \leqslant J^c_{1b}$, the energies of the two configurations are believed to be the same. The J^c_{1b} decreases with the increase of anisotropy. When $J_{1b} = 0.7$, it is seen that $F_{\mathrm{AF1}}(0^+) < F_{\mathrm{AF2}}(0^+)$, indicating that AF1 is more stable near zero temperature. Since F_{AF2} drops faster than F_{AF1}, the two curves have a cross point when temperature increases to a certain value. It means that there can occur an AF1-AF2 phase transition at the cross point. However, their internal energies differ. Therefore, it is a first-order transition. Above the transition point, the AF2 is more stable until the Néel point T_N. As J_{1b} further increases, F_{AF2} is always lower than F_{AF1}. In this case, the AF2 is more stable and there is no phase transition.

In the following, the stability of the two states will be discussed for fixed J_{1b} while D changes. Figure 5(a) plots the $F(T)$ curves for different D values when $J_{1b} = 0.5$. To be explicit, Fig. 5(b) plots the enlargements for $D = 0.001$ and 0.01 and Fig. 5(c) for $D = 0.08$, respectively. As D increases from 0.001 to 0.01, F_{AF2} is always less than F_{AF1} below the Néel point, indicating that the AF2 is more stable. However, the difference between $F_{\mathrm{AF1}}(0^+)$ and $F_{\mathrm{AF2}}(0^+)$

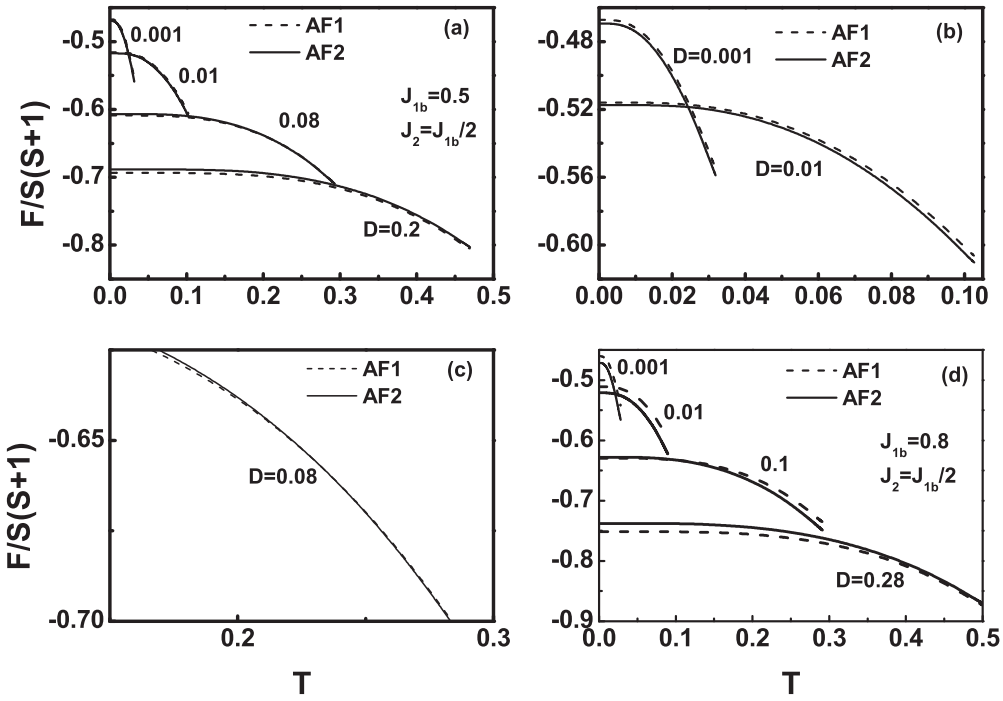

FIG. 5. (a) The free energies $F(T)$ as a function of temperature T for different D values when $J_{1b} = 0.5$. (b) The enlargement of (a) in the case of $D = 0.001$ and 0.01. (c) The enlargement of the region of the free-energy curves near cross point when $D = 0.08$. (d) The free energies $F(T)$ as a function of temperature T for different D values when $J_{1b} = 0.8$.

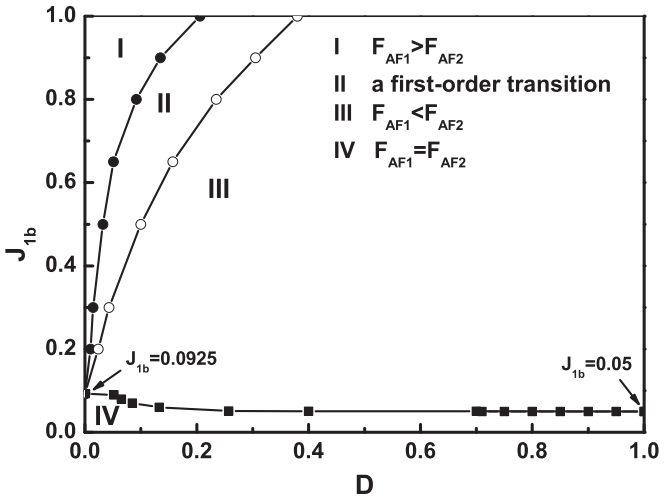

FIG. 6. The comparison of the free energies of the two states below the T_N in the J_{1b} and D parameter space.

decreases with increasing D. When D is greater than 0.08, $F_{\mathrm{AF1}}(0^+) < F_{\mathrm{AF2}}(0^+)$, which means that the AF1 is more stable. Moreover, the curves of the free energies of the AF1 and AF2 have a cross point, at which a phase transition can occur between the two states. This is a first-order transition. Above the transition point, the AF2 is more stable until T_N. When D further increases, F_{AF1} is always lower than F_{AF2} within the whole range of temperatures below the critical point. In this case, the AF1 is more stable. As a comparison, Fig. 5(d) plots the free energy as a function of temperature at $J_{1b} = 0.8$. The results are similar to those in Fig. 5(a).

Now, we present a comprehensive recognition of the effect of parameters J_{1b} and D on the free energies of the two states below the T_N. Figure 6 shows the comparison of the free energies between the two states in the whole temperature range below the T_N. It is seen that there are four regions. In region I, the free energy of the AF1 state is always greater than that of the AF2. The examples are the curves in Figs. 3(c) and 3(d). This region is denoted as $F_{\mathrm{AF1}} > F_{\mathrm{AF2}}$. In region II, at temperatures close to zero, $F_{\mathrm{AF1}}(0^+) < F_{\mathrm{AF2}}(0^+)$, and near the T_N $F_{\mathrm{AF1}}(T) > F_{\mathrm{AF2}}(T)$. Therefore, there is a first-order transition below the T_N. The examples are the curve with $J_{1b} = 0.7$ in Fig. 4 and that with $D = 0.1$ in Fig. 5(d). In region III, which is denoted by $F_{\mathrm{AF1}} < F_{\mathrm{AF2}}$, the free energy of the AF1 state is always lower than that of the AF2. The examples at the curve in Fig. 5(a) with $D = 0.2$ and that in Fig. 5(d) with $D = 0.28$. In region IV, the difference of the free energies of the two states is negligible. So it is denoted as $F_{\mathrm{AF1}} = F_{\mathrm{AF2}}$. The examples are the curves in Figs. 3(a) and 3(b).

Roughly speaking, when J_{1b} value is very small, in region IV, the free energies of the two states are very close to each other and one cannot tell which is more stable. When the J_{1b} value is not very small, with the increase of the D value, the case of $F_{\mathrm{AF1}} > F_{\mathrm{AF2}}$ gradually transits to the case $F_{\mathrm{AF1}} < F_{\mathrm{AF2}}$.

C. Possible phase transition at $J_2 \neq J_{1b}/2$

Figure 7 plots the free energy as a function of temperature for $D = 0.05$. For $J_{1b} = 0.05$ [i.e., Figs. 7(a) and 7(b)], we distinguish two cases where $J_2 < 0.025$ and $J_2 > 0.025$, respectively. Figure 7(a) plots the curves of $J_2 = 0.022$ and 0.024, and Fig. 7(b) the curves of $J_2 = 0.026$ and 0.028. For the former case, the critical temperature of AF1 is higher than AF2, while it is contrary for the latter case, which is also reflected in Fig. 2(c). In the former case, $F_{\mathrm{AF1}}(0^+)$ is always

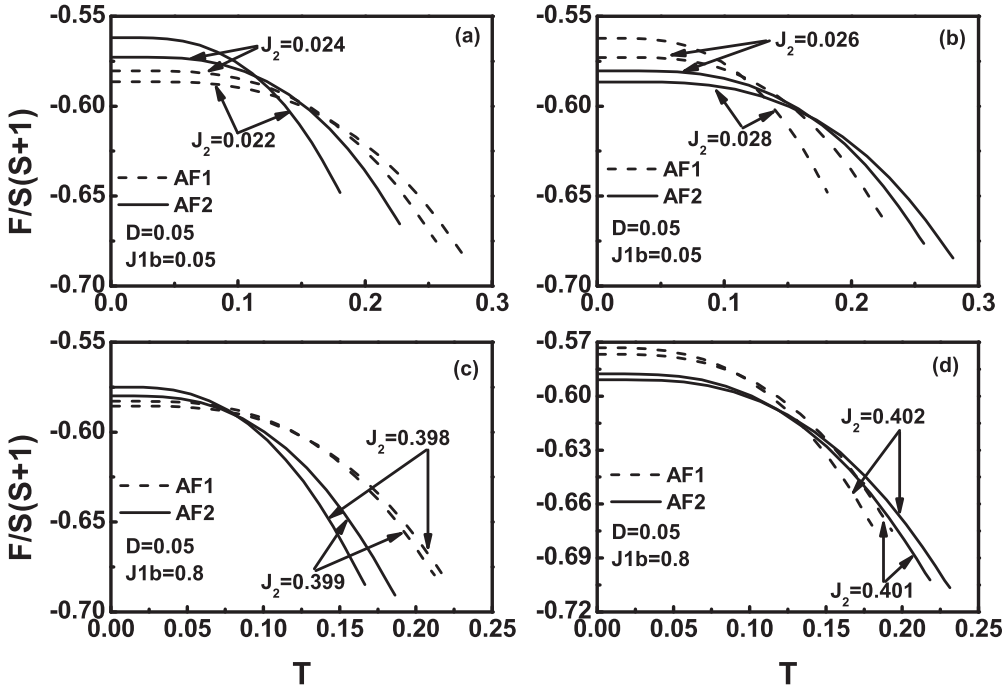

FIG. 7. The free energies $F(T)$ as a function of the temperature T at $D = 0.05$. (a) $J_{1b} = 0.05$ and $J_2 = 0.022, 0.024$; (b) $J_{1b} = 0.05$ and $J_2 = 0.026, 0.028$; (c) $J_{1b} = 0.8$ and $J_2 = 0.398, 0.399$; and (d) $J_{1b} = 0.8$ and $J_2 = 0.401, 0.402$.

less than $F_{AF2}(0^+)$. It indicates that AF1 is more stable near zero temperature. The free-energy curves of the two states cross at a temperature. At the cross point, an AF1-AF2 phase transformation may occur. It is a first-order transition, as the internal energy has a jump. Above the cross point, $F_{AF1} > F_{AF2}$ so the AF2 is more stable. The latter case is contrary to the former, i.e., AF2 is more stable near zero temperature, and above the cross point, the AF1 is more stable. For $J_{1b} = 0.8$, the case where $J_2 < 0.4$ shown in Fig. 7(c) is similar to that in Fig. 7(a), and the case where $J_2 > 0.4$ is similar to that in Fig. 7(d). The boundary of the two cases is always $J_2 = J_{1b}/2$.

Figure 7 indicates that, for the case of $J_2 \neq J_{1b}/2$, the higher the T_N, the lower the $F_{AF2}(0^+)$, and the decreasing of the $F(T)$ curve becomes slower. From the discussion above, three conclusions can be drawn. (1) The free-energy curves of the two states cross, i.e., a transition transformation between the two states may occur. (2) At low temperature, the state with the higher critical temperature is more stable, and at high temperature, the state with the lower critical temperature is more stable. (3) Under the same parameters, the larger the difference between the T_N's of the AF1 and AF2 states, the larger the difference between $F_{AF1}(0^+)$ and $F_{AF2}(0^+)$.

IV. CONCLUDING REMARKS

In this paper, the phase transition of the quantum spin-1 anisotropic Heisenberg antiferromagnet on a square lattice has been studied by the double-time Green's function method. The stability of AF1 and AF2 has been discussed in detail by comparing their free energies. Two cases of $J_2 = J_{1b}/2$ and $J_2 \neq J_{1b}/2$ are discussed separately.

For the case of $J_2 = J_{1b}/2$, our comprehensive results are shown in Fig. 6. When J_{1b} value is very small, as in region IV in Fig. 4, one could not tell which of AF1 and AF2 is more stable, so their coexistence is possible. When J_{1b} value is not very small and the D value is within a narrow range, a first-order transition below the Néel point could occur. Otherwise, the free energy of one of the two states is always lower than another in the whole temperature range below the T_N.

When $J_2 \neq J_{1b}/2$, although both states may also exist, their critical temperatures differ. For $J_2 < J_{1b}/2$ ($J_2 > J_{1b}/2$), the critical temperature of the AF1 (AF2) state is higher than that of AF2 (AF1). Meanwhile, the AF1 (AF2) is more stable near zero temperature, and AF2 (AF1) is more stable near T_N. Therefore, at an intermediate temperature, a first-order phase transition between these two states may occur.

ACKNOWLEDGMENTS

This work was supported by the 973 Project of China (Grant No. 2012CB927402) and the National Natural Science Foundation of China (Grants No. 61275028 and No. 11404046).

[1] G. Misguich and C. Lhuillier, in *Frustrated Spin Systems*, edited by H. T. Diep (World Scientific, Singapore, 2004).
[2] R. Coldea, S. M. Hayden, G. Aeppli, T. G. Perring, C. D. Frost, T. E. Mason, S.-W. Cheong, and Z. Fisk, Phys. Rev. Lett. **86**, 5377 (2001).
[3] P. Carretta, N. Papinutto, C. B. Azzoni, M. C. Mozzati, E. Pavarini, S. Gonthier, and P. Millet, Phys. Rev. B **66**, 094420 (2002).
[4] R. Melzi, P. Carretta, A. Lascialfari, M. Mambrini, M. Troyer, P. Millet, and F. Mila, Phys. Rev. Lett. **85**, 1318 (2000).
[5] E. Pavarini, S. C. Tarantino, T. B. Ballaran, M. Zema, P. Ghigna, and P. Carretta, Phys. Rev. B **77**, 014425 (2008).
[6] R. Melzi, S. Aldrovandi, F. Tedoldi, P. Carretta, P. Millet, and F. Mila, Phys. Rev. B **64**, 024409 (2001).
[7] A. Bombardi, J. Rodriguez-Carvajal, S. Di Matteo, F. de Bergevin, L. Paolasini, P. Carretta, P. Millet, and R. Caciuffo, Phys. Rev. Lett. **93**, 027202 (2004).
[8] Chung-Pin Chou and Hong-Yi Chen, Phys. Rev. B **90**, 041106(R) (2014).
[9] J. Richter and J. Schulenburg, Eur. Phys. J. B **73**, 117 (2010).
[10] O. Götze, S. E. Krüger, F. Fleck, J. Schulenburg, and J. Richter, Phys. Rev. B **85**, 224424 (2012).
[11] R. Darradi, O. Derzhko, R. Zinke, J. Schulenburg, S. E. Krüger, and J. Richter, Phys. Rev. B **78**, 214415 (2008).
[12] R. L. Doretto, Phys. Rev. B **89**, 104415 (2014).
[13] Shou-Shu Gong, Wei Zhu, D. N. Sheng, Olexei I. Motrunich, and Matthew P. A. Fisher, Phys. Rev. Lett. **113**, 027201 (2014).
[14] O. P. Sushkov, J. Oitmaa, and Z. Weihong, Phys. Rev. B **63**, 104420 (2001).
[15] X. G. Wen, Phys. Rev. B **44**, 2664 (1991).
[16] Guang-Ming Zhang, Hui Hu, and Lu Yu, Phys. Rev. Lett. **91**, 067201 (2003).
[17] T. Roscilde, A. Feiguin, A. L. Chernyshev, S. Liu, and S. Haas, Phys. Rev. Lett. **93**, 017203 (2004).
[18] R. F. Bishop, P. H. Y. Li, R. Darradi, J. Schulenburg, and J. Richter, Phys. Rev. B **78**, 054412 (2008).
[19] A. Metavitsiadis, D. Sellmann, and S. Eggert, Phys. Rev. B **89**, 241104(R) (2014).
[20] O. D. Mabelini, O. D. R. Salmon, and J. Ricardo de Sousa, Solid State Commun. **165**, 33 (2013).
[21] P. Sindzingre, Phys. Rev. B **69**, 094418 (2004).
[22] K. Majumdar, D. Furton, and G. S. Uhrig, Phys. Rev. B **85**, 144420 (2012).
[23] R. F. Bishop, P. H. Y. Li, R. Darradi, and J. Richter, Europhys. Lett. **83**, 47004 (2008).
[24] R. F. Bishop, P. H. Y. Li, R. Darradi, and J. Richter, J. Phys.: Condens. Matter **20**, 255251 (2008).
[25] K. Takasaki, T. Tonegawa, and M. Kaburagi, J. Phys. Soc. Jpn. **57**, 570 (1988).
[26] N. D. Mermin and H. Wagner, Phys. Rev. Lett. **17**, 1133 (1966).
[27] Huai-Yu Wang, *Green's Function in Condensed Matter Physics*, (Alpha Science International Ltd. and Science Press, Beijing, 2012).
[28] P. Fröbrich, P. J. Jensen, and P. J. Kuntz, Eur. Phys. J. B **13**, 477 (2000).
[29] P. Fröbrich and P. J. Kuntz, Phys. Rep. **432**, 223 (2006).
[30] Huai-Yu Wang, Liang-Jun Zhai, and Meichun Qian, J. Magn. Magn. Mater. **354**, 309 (2014).